Numerical simulations of Pelton turbine flow to predict large head variation influence

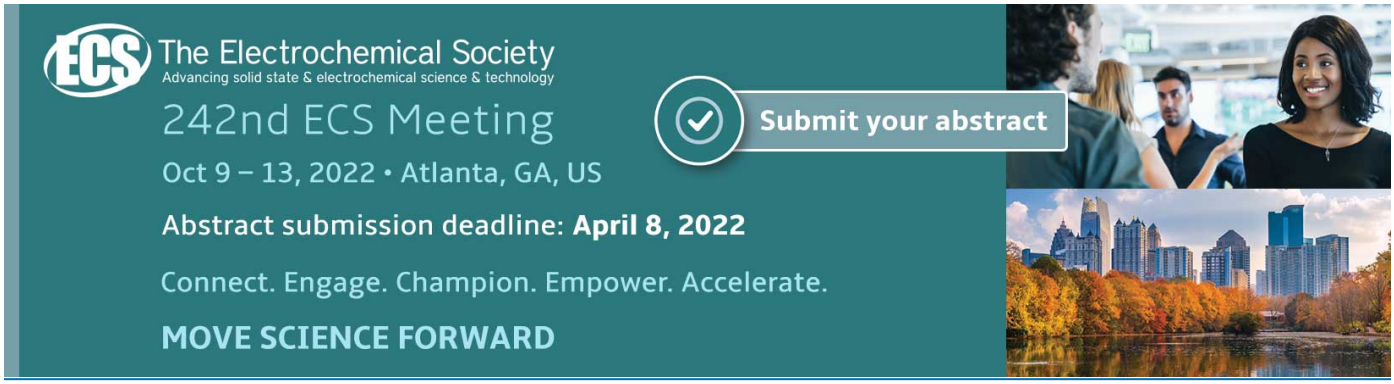

Numerical simulations of Pelton turbine flow to predict large head variation influence

S Alimirzazadeh[1*], J Decaix[2], F Avellan[1], S. Crettenand[3], C. Münch-Alligné[2]

[1] Laboratory for Hydraulic Machines, École Polytechnique Fédérale de Lausanne, Lausanne, Switzerland
[2] Institute of Sustainable Energy, School of Engineering, HES-SO Valais-Wallis, Switzerland
[3] Forces Motrices Vaaisannes FMV, Sion, Switzerland

*siamak.alimirzazadeh@epfl.ch

Abstract. In the framework of the new feed-in-tariff system in Switzerland for Small Hydropower Plants (SHP), the aim of the SmallFLEX project, led by HES-SO Valais and performed in collaboration with EPFL, WSL, EAWAG, PVE, and FMV, is to show how SHP can provide winter peak energy and ancillary services, whilst remaining eco-compatible. The pilot and demonstrator site selected is the new small hydropower plant of Gletsch-Oberwald (KWGO) owned by FMV and commissioned end of 2017. This run-of-river power plant is equipped with two six-jet Pelton turbine units featuring a maximum power of 7 MW each.
The addition of flexibility can be reached by using existing volumes of the power plant: the settling basin, the forebay chamber as well as part of the headrace tunnel. By consequence, the turbine head will undergo variations. To ensure that these variations will not cause any damages to the Pelton runner, the influence of the available head is investigated by numerical simulations. The simulations are carried out using two different software. OpenFOAM, which is based on a Finite Volume Method (FVM), is used for computing the flow inside the distributor until the jet. GPU-SPHEROS, which is based on Arbitrary Lagrangian-Eulerian (ALE) Finite Volume Particle Method (FVPM) is utilized to compute the interaction between the jet and Pelton buckets.
Mixing the two aforementioned approaches, i.e. mesh-based FVM and particle-based FVPM, the overall torque T of the present six-jet Pelton runner can be reconstructed for different rated heads and discharges. The predicted torque fluctuations can then be considered for an estimation of the structural fatigue damage of the runner.

1. Introduction

In the current trend of the electricity market, the flexibility of the production is more and more required. Switzerland has adapted its legislation in 2018 by changing the feed-in-tariff system [1]. One of the consequences is the requirement to produce the right amount of power at the right time. For small run-off river power plants, such a requirement is challenging to tackle. In the framework of the SmallFLEX project, led by HES-SO Valais and performed in collaboration with EPFL, WSL, EAWAG, PVE, and FMV, the goal is to show how Small Hydropower Plant (SHP) can provide winter peak energy and ancillary services, whilst remaining eco-compatible. The chosen pilot site is the new small hydropower plant of Gletsch-Oberwald (KWGO) owned by FMV and commissioned end of 2017. This run-of-river power plant is equipped with two six-jet Pelton turbine units featuring a maximum power of 7 MW each.

The increase in flexibility for this power plant can be achieved by using all the storage volumes available such as the settling basin, the forebay chamber, and part of the headrace channel [2]. However, the use of such volumes will lead to operating the Pelton turbines under various head values, for which they are not specifically designed.

Numerical simulations are performed to investigate the influence of the head on the quality of the jet and the torque. The quality of the jet is a key feature for the operation of the turbine [3] and can influence the fatigue

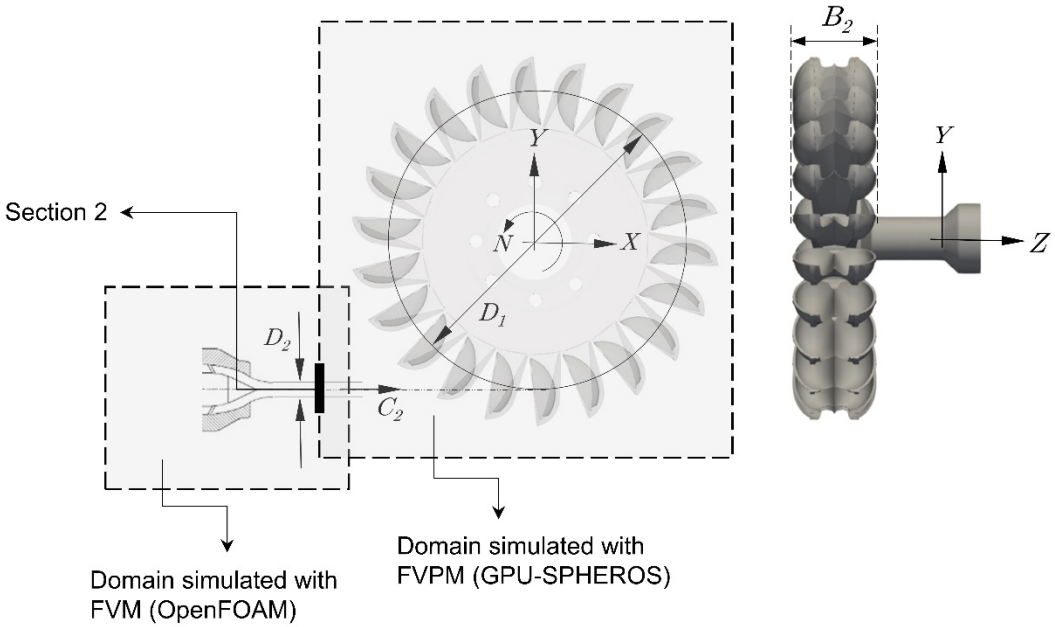

Figure 1. Domains simulated with the mesh-based and particle-based method. The data in section 2 is extracted from the mesh-based simulation which is performed with OpenFOAM to be used as an inlet for particle-based simulation performed with GPU-SPHEROS.

and the efficiency of the runner. However, the physics of the flow in a Pelton turbine is very complex [4] since it involves both a single-phase internal flow inside the distributor and a free surface flow inside the casing. Besides, the flow is characterized by the presence of high velocity and density gradients. Finally, the jet interacts with a rotating part, i.e. the runner and themselves. All these features are not straightforward to be captured by using only one numerical tool, e.g. a mesh-based Eulerian solver [5].

In the present work, a Finite Volume Method (FVM), provided by the OpenFOAM toolbox, is used to compute the flow from the distributor to the jet without considering the buckets. Then, an Arbitrary Lagrangian-Eulerian (ALE) Finite Volume Particle Method (FVPM) accelerated by GPU is utilized to investigate the interaction between the jets and the buckets and computing the torque recovered by the runner (see Figure 1). The solver is called GPU-SPHEROS developed in EPFL-LMH since 2015. The reader is referred to [6], [7], [8], [9], and [10] for more information regarding GPU-SPHEROS development and implementations.

2. Numerical tools

2.1. OpenFOAM

The OpenFOAM toolbox provides several Reynolds-Averaged Navier-Stokes (RANS) solvers based on an FVM framework. The interFoam solver allows for computing turbulent two-phase flows without phase change. For the present test case, this solver is used to compute the Pelton water jet from the inlet of the nozzle to an arbitrary outlet box (see Figure 2).

The mesh is almost hexahedral generated with snappyHexMesh tool provided by the OpenFOAM toolbox. The number of cells is slightly above 5 million and wall layers are added along the no-slip walls to capture the boundary layer accurately. Specific refinements are imposed in the nozzle outlet region.

The turbulence effects are modeled with the standard SST k-ω model and the total pressure corresponding to the targeted head and the liquid volume fraction are imposed at the inlet of the nozzle. No-slip walls are

specified for the internal walls of the nozzle. On the contrary, free-slip walls are specified for the surrounding walls of the outlet box excepted at the outlet section where the static pressure is imposed. Therefore, the discharge Q is an output of the simulation.

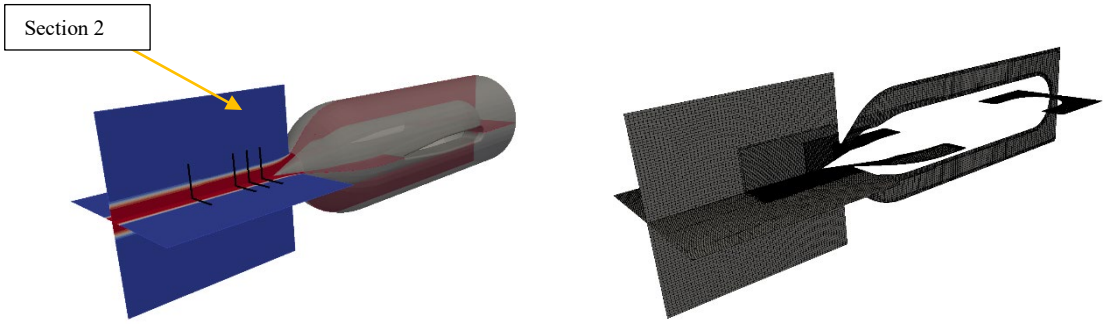

Figure 2. View of the computational domain (left) and the generated mesh (right) used to compute the Pelton water jet with OpenFOAM.

2.2. GPU-SPHEROS

GPU-SPHEROS is based on FVPM discretized equations [6] that can be interpreted as a generalization of the conventional mesh-based FVM. In FVM, the computational domain is partitioned into finite control volumes with defined surfaces. The area vector of the surfaces is used as a weight for the flux exchanged between the control volumes. In FVPM, control volumes are replaced by overlapping particles and the exchange occurs through the interfaces defined by overlapping regions. For each pair (i,j) of overlapping particles (referred to as neighbors), two interaction vectors $\mathbf{\Gamma}_{ij}$ and $\mathbf{\Gamma}_{ji}$ are defined and their difference $\mathbf{\Delta}_{ij} = \mathbf{\Gamma}_{ij} - \mathbf{\Gamma}_{ji}$ is analogous to the area vector in FVM. Readers are referred to [1] and [7] for more details.

The method has also been developed, implemented, and accelerated on Graphics Processing Unit (GPU) as a particle-based conservative and consistent fluid solver. The solver is called GPU-SPHEROS and has been already validated against the experimental data for an impinging jet on a flat plate and a Pelton turbine. The reader is referred to [10] and [11] for more details on GPU-SPHEROS validation.

The schematic of a six-jet Pelton runner simulation setup is shown in Figure 3. The buckets rotate about the Z-axis and θ is the angle between the intermediate bucket and the Y-axis. The six-jet simulation setup is simplified by injecting only two adjacent jets with an angle of 60° between them to decrease the computational cost by taking advantage of geometric periodicity.

For the two jets, the discharge velocity of the water jet, as well as turbulence variables including turbulence kinetic energy k and turbulence dissipation rate ε, are imposed using the solution of the OpenFOAM simulations in section 2 (see Figure 2). Since there is no volume fraction parameter in GPU-SPHEROS as a single-phase FVPM solver, the particles' velocity profile extracted from the FVM solution is weighted by the water volume fraction and the jet diameter is then found in the sense of having the same water discharge as the OpenFOAM data. Since the velocity profile is changed by weighting the velocity by volume fraction keeping the momentum the same as water jet momentum computed with OpenFoam, the discharge will be different. However, for the torque computations, the water jet momentum is kept conserved rather than the discharge. The standard k-ε model is implemented and utilized in GPU-SPHEROS to model the turbulence effects. The simulations have been performed for different heads and discharges (see Table 1). An example of the inlet particles is shown in Figure 4. The particle size for the simulation is chosen based on the previous convergence study performed in [11]. For the largest jet diameter, i.e. the largest discharge and needle stroke, the inlet boundary has $D_2 / X_{ref} = 30$ particles to provide acceptable accuracy in a reasonable time. D_2 is the jet diameter and X_{ref} is the distance between two adjacent particles. Although the jet diameter is changed with the change in nozzle stroke opening

S and discharge *Q*, the particle size is kept identical for all the simulations to have the same spatial discretization error. The reader is referred to [11] for more details on the convergence study.

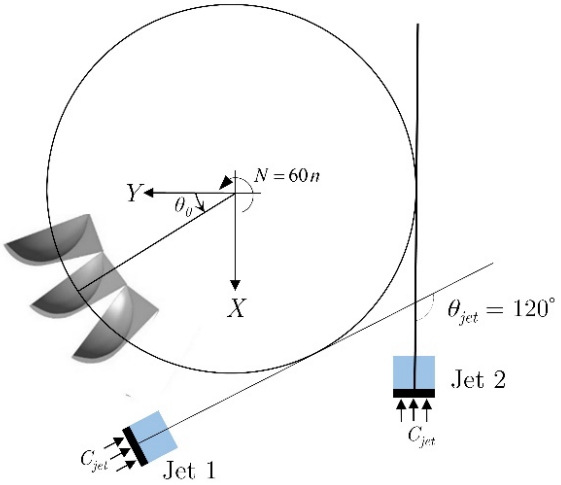

Figure 3. Simplified double-jet numerical simulation setup with only two adjacent jets with 60° between them. θ is the angle between the middle bucket and the *Y*-axis.

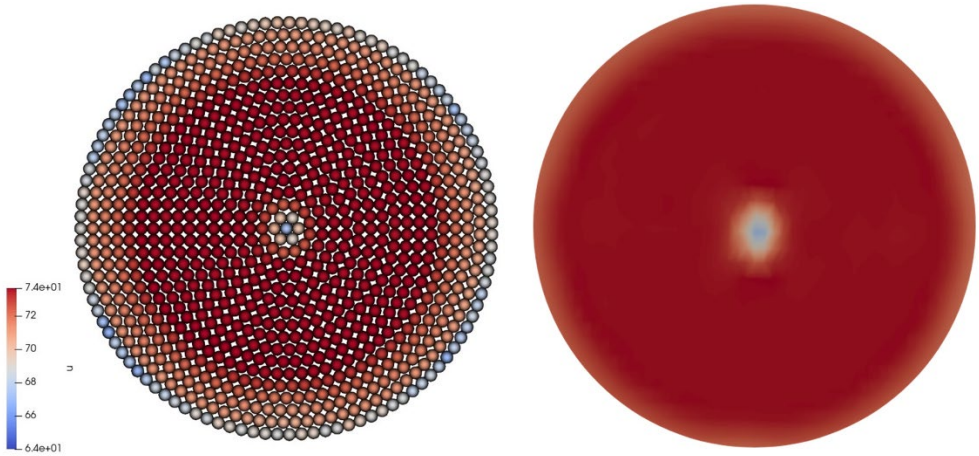

Figure 4. The velocity profile computed with OpenFOAM (right) and the corresponding extracted profile used as inlet boundary in GPU-SPHEROS (left).

3. Results

3.1. Operating points and jet velocity profile

12 operating points are considered covering four different heads. i.e. H/H_{max}= 1.0, 0.888, 0.749, 0.662 and three different needle stroke openings, i.e. 20%, 49%, and 90%. The four heads correspond to the maximum head, the lowest possible head in the settling basin keeping the headrace tunnel filling by water, and two lower heads corresponding to a partial emptying of the headrace tunnel.

In Table 1, for each simulation, the discharge is compared with the discharge extracted from the Hydro-Clone of the power plant (provided by Power Vision Engineering[1], one of the partners of the project). The relative difference between the two approaches is lower than ±2.5%.

[1] http://www.powervision-eng.ch/hydro-clone-software/

Table 1. Simulated operating points and predicted discharges. OpenFOAM simulations.

Case#	S [%]	H/H_{max} [-]	Q/Q_{max} [-] *CFD*	Q/Q_{max} [-] *Hydro-Clone*	The relative difference [%]
1	20	1.0	0.343	0.332	2.4
2		0.982	0.339	0.328	2.4
3		0.958	0.335	0.324	2.3
4		0.888	0.322	0.312	2.2
5	49	1.0	0.704	0.700	-0.5
6		0.982	0.697	0.694	-0.8
7		0.958	0.687	0.685	-0.8
8		0.888	0.662	0.660	-0.8
9	90	1.0	1.0	1.0	-1.0
10		0.982	0.989	0.989	-1.1
11		0.958	0.978	0.978	-1.1
12		0.888	0.939	0.942	-1.3

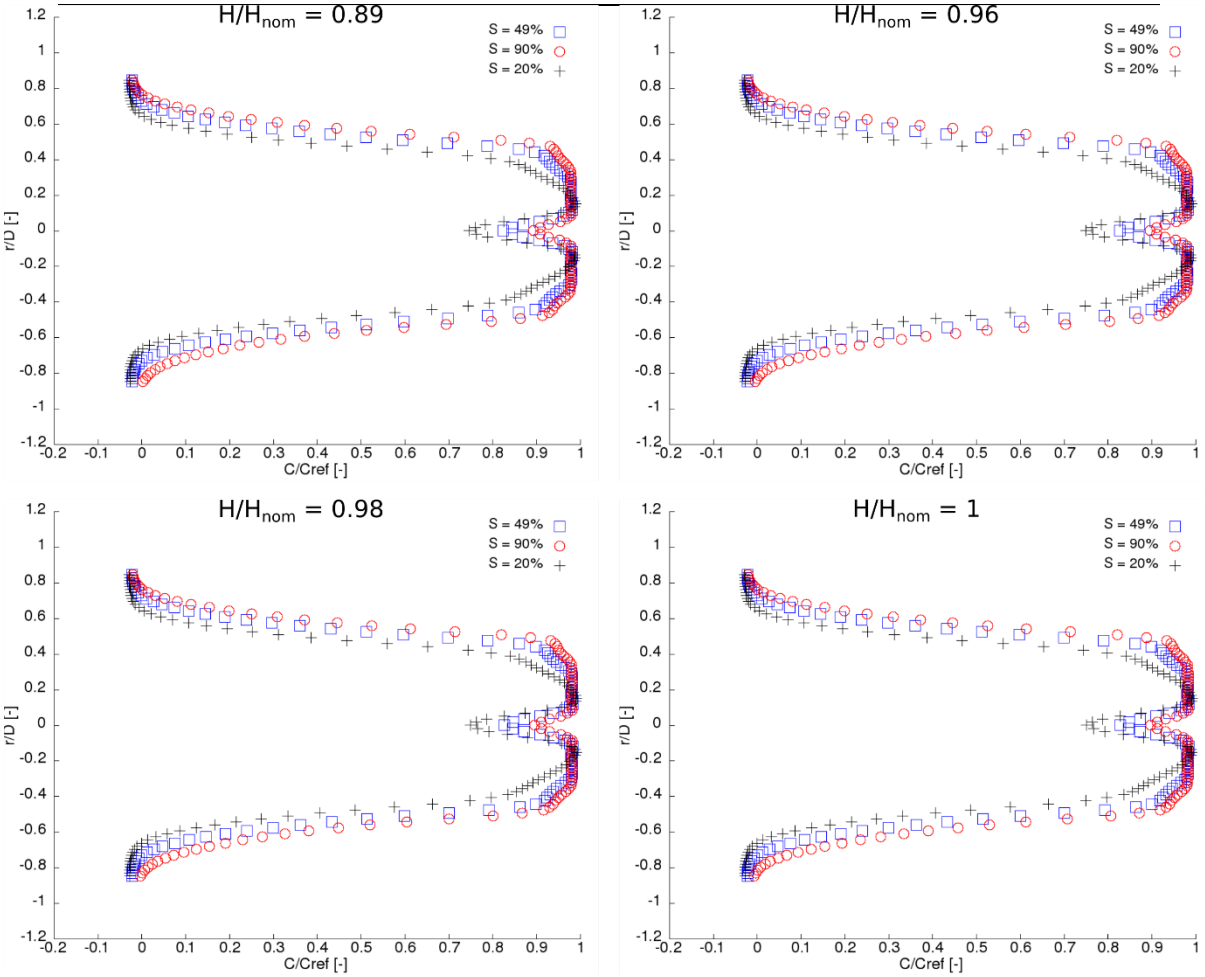

Figure 5. The axial jet velocity profile in section 2 for each operating point provided by OpenFOAM simulation.

The axial jet velocity profiles in section 2, located at 1.42 × D_{nozzle} downstream of the nozzle outlet, are plotted in Figure 5 for each operating point. For each head, the maximum velocity agrees with the

Torricelli formula. The reference velocity C_{ref} is the velocity that is set at the distributor inlet based on the inlet discharge Q_{inlet}. By increasing the opening of the needle stroke, the velocity deficit in the wake of the needle valve decreases, it reaches 20% of the maximum velocity for the smallest opening and only 8% for the largest opening. Also, the span of the jet increases slightly by increasing the opening.

3.2. Torque time-history and torque fluctuations

The runner torque time-history computations are then performed with GPU-SPHEROS with the velocity profiles extracted from the OpenFOAM simulations in section 2 as inlet boundary conditions.

The interaction between the two jets and the three runner buckets is illustrated in Figure 6. In a Pelton runner, the interaction between the jet and bucket can be decomposed along the following stages. First, the jet interferes with the bucket at the splitter tip zone. The water jet is then split by the splitter tip and cutout zone and starts to impact the internal surface of the bucket. An immediate primary jump in torque time-history can be seen which corresponds to the beginning of this impact moment. Part of the water jet then enters the adjacent bucket in the next stage. However, the jet still enters the current bucket and torque reaches its maximum value, i.e. the peak. By increasing the angle between the jet and bucket, the jet starts to evacuate the bucket, and the torque is gradually decreased. The dimensionless torque factor time-history $k_T = T/0.5\rho D_1^3 C_2^2$ against the bucket angular position is shown in Figure 7. T, D_1, and C_2 are the torque, runner diameter, and jet velocity, respectively, and ρ is the water density. As can be seen, the torque generated by jet 2 is affected by the flow injected by jet 1 which is not entirely discharged when the next jet enters. The magnitude of the torque peak increases for higher head values since a larger momentum is transferred by the water to the runner when the rated head is higher. The Savitzky-Golay filter is utilized to fit a smooth curve from the raw data.

The sudden jump shown in torque time-history can cause high-amplitude torque fluctuations. The magnitude of this jump is affected by the bucket geometry. The geometry, especially around the cutout, can splash and disturb the water flow when the jet is cut by the splitter entering the bucket. The disturbed water particles cannot catch up with the bucket as if they are jumping and the torque suddenly increases when these water particles land and impact the internal surface of the bucket. This is intensified by increasing the nozzle opening size since the jet diameter increases and a larger momentum is contributed to those disturbed particles impacting the bucket surface. For smaller jet diameters, this phenomenon is weakened. The large jump in torque can lead to large torque fluctuations.

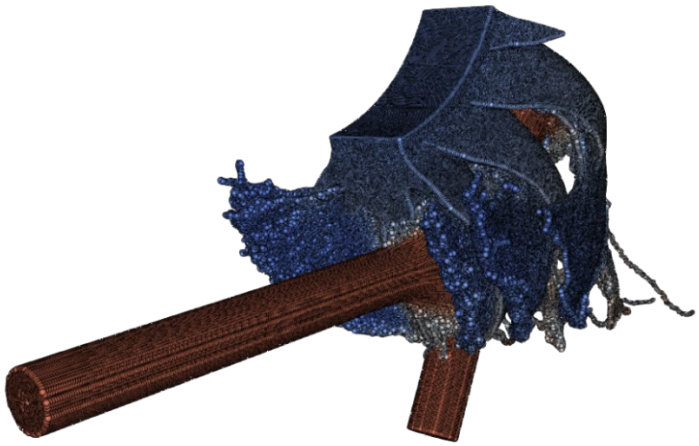

Figure 6. Water particles deviated by rotating Pelton buckets. GPU-SPHEROS simulation.

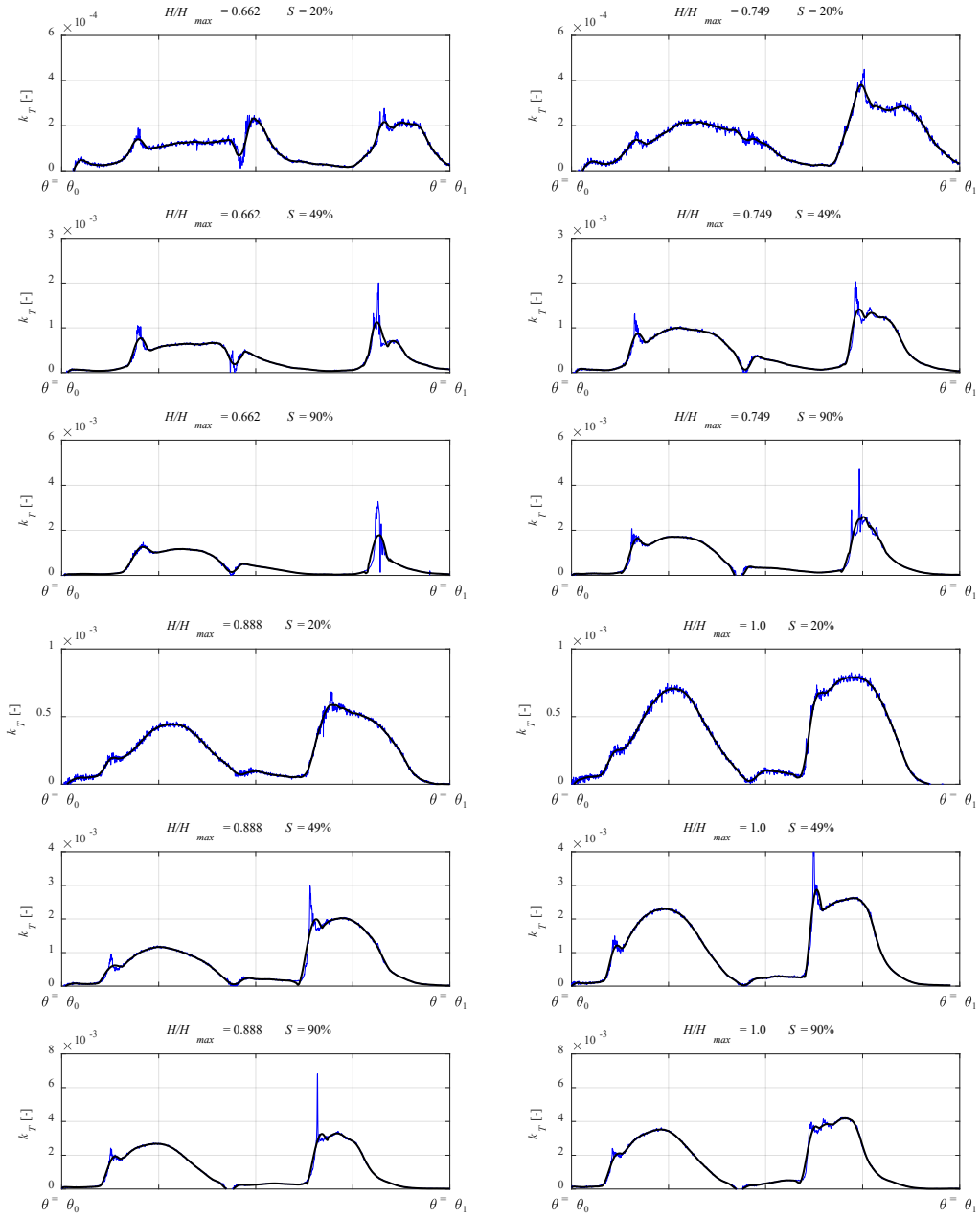

Figure 7. The middle bucket torque time-history for the 12 operating points. The black curve is fitted from the raw data in blue using the Savitzky-Golay filter.

The overall torque time-history is also computed for all the operating points to assess the effect of head H and discharge Q variations on torque fluctuations. The results are shown in Figure 8, which are based on time-shifted and superimposed torque copies of jet 2 in which the effect of jet interference and disturbance are covered. The time-averaged torque and the amplitude of the fluctuations for each case are shown in Figure 9. The time-averaged torque is increased by increasing the rated head and the torque fluctuations amplitude is intensified by increasing the needle stroke opening for larger discharges. The larger torque fluctuations are due to a larger jump in torque time-history for larger jet diameters. A similar trend for torque fluctuations is shown

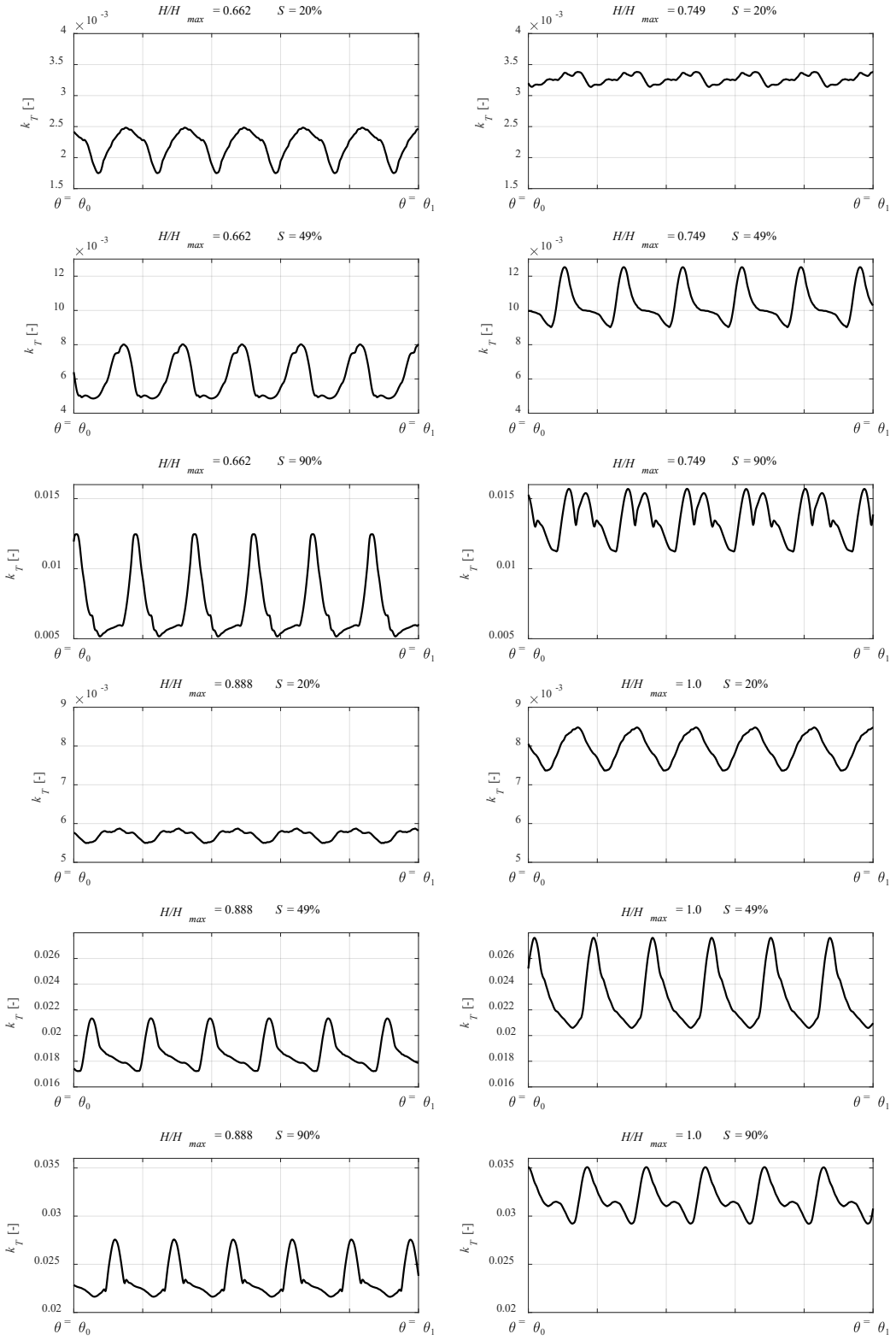

Figure 8. The computed overall torque time-histories of the six-jet Pelton based on the isolated torque time-history generated by jet 2.

by Perrig et al. [13] validated by experimental results. Installing pressure sensors inside the bucket to measure the pressure fluctuations can be a reliable way to validate the present results.

Since the torque fluctuations are equivalent to pressure fluctuations, the stress, which is the most important factor in fatigue damage, is intensified with higher torque fluctuations. Although the number of cycles required to cause fatigue failure at particular peak stress is significantly high, it decreases when the stress amplitude is increased [12]. Therefore the torque fluctuations amplitude is directly linked to structural fatigue and higher fluctuations will significantly accelerate the fatigue damage process in the runner. Nevertheless, the fluctuations predicted with the simulations seem to be higher than expected and should be taken with caution. A comparison with experimental results will be necessary to confirm the observations. Numerical instabilities linked to the capacity of the numerical scheme to capture the shock generated by the jet impact must be first excluded.

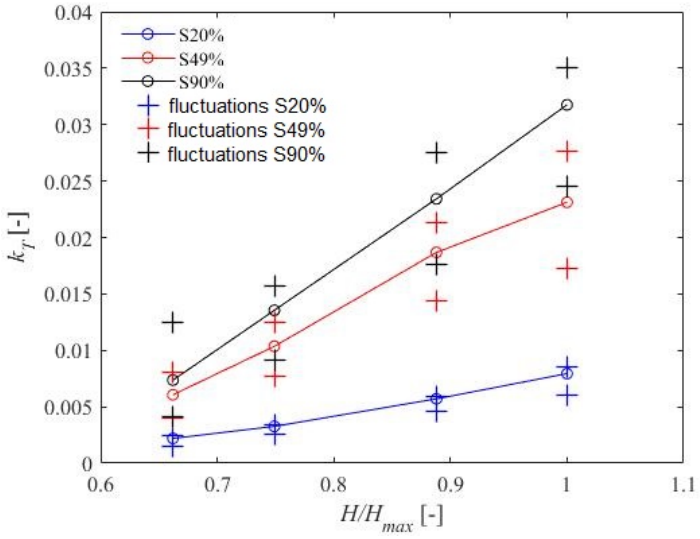

Figure 9. Time-averaged torque and fluctuations amplitude for different heads and needle stroke opening size.

4. Conclusion

In the framework of the SmallFLEX project, the effect of large head variations on the jet velocity and torque time-history of a Pelton turbine has been studied considering 12 operating points varying the rated head and the nozzle stroke opening. OpenFOAM was used for the turbulent internal flow simulation inside the nozzle and compute the jet velocity profiles at different operating points. The results have been used as input for particle-based simulations of the interactions between the jets and buckets. As a particle-based solver, GPU-SPHEROS is robust to handle rotating Pelton turbine simulation as a free-surface problem with large deformations in boundaries, in which the mesh-based methods can face difficulty. Mixing the two approaches provides the ability of a full Pelton turbine simulation.

The internal flow inside the nozzle, as until the injected jet, have been simulated using OpenFOAM mesh-based solver to compute the discharge and predict the water velocity profiles for 12 operating conditions. For the free surface part where the jet is injected from the nozzle on the runner, the VOF method has been used for air-water two-phase flow simulation with the OpenFOAM solver. The extracted velocity profiles computed by OpenFOAM have been used as an inlet boundary for GPU-SPHEROS simulations to predict the bucket torque time-history for each operating point. The overall torque is then computed based on the torque generated by jet 2 in which the effect of any interference between the adjacent jets is covered.

The results show that by increasing the opening of the needle stroke, the velocity deficit in the wake of the needle valve decreases, reaching 20% of the maximum velocity for the smallest opening and only 8% for the largest opening. Also, the span of the jet increases slightly by increasing the opening.

Moreover, the torque fluctuations amplitude is significantly intensified by increasing the needle stroke opening. High torque fluctuations have been observed and must be confirmed by comparison with measurements. which are mostly due to a sudden jump in bucket torque time-history which becomes larger for larger jet diameters. Such torque fluctuations can significantly accelerate the fatigue damage process in the runner applying repair and outage costs. The computed torque fluctuations amplitude and frequency can be used for runner fatigue analysis.

Acknowledgments
This study is part of the SmallFLEX project granted by the Swiss Federal Office of Energy (OFEN no. SI/501636-01) and financially and technically supported by Forces Motrices Valaisannes (FMV).

Reference
[1] Loi fédérale du 30 septembre 2016 sur l'énergie (LEne).
[2] Zordan J, Manso P.A, Gaspoz A, Münch C, Crettenand S, 2019, Introducing flexibility in alpine small hydropower plants using smart storage, *Hydro 2019 conference*, Porto, Portugal.
[3] Peron M, Parkinson E, Geppert L, Thomas S, 2008, Importance of jet quality on Pleton efficiency and cavitation, *In International Conference on Hydraulic Efficiency Measurements* - IGHEM 2008 - Milano 3rd-6th September p. 1–9.
[4] Sick M, Keck H, Vuilloud G, Parkinson E, 2000, New challenges in Pelton research, *Hydro 2000 conference*, Bern, Switzerland
[5] Audrius Ž, Aggidis G. A, 2015, State of the art in numerical modeling of Pelton turbines. *Renewable and Sustainable Energy Reviews*, ***45***, 135–144.
[6] Jahanbakhsh E, Vessaz C, Maertens A, Avellan F, 2016, Development of a Finite Volume Particle Method for 3-D fluid flow, *Computer Methods in Applied Mechanics and Engineering*, **298**, pp. 80-107.
[7] Jahanbakhsh E, Maertens A, Quinlan N J, Vessaz C, Avellan F, Exact finite volume particle method with spherical-support kernels, *Computer Methods in Applied Mechanics and Engineering*, **317** (2017) 102–127.
[8] Vessaz C, 2015, Finite Particle Flow Simulation of Free Jet Deviation by Rotating Pelton Buckets, *École Polytechnique Fédérale de Lausanne (EPFL) doctoral thesis* N° **6470**.
[9] Vessaz C, Jahanbakhsh E, Avellan F, 2015, Flow Simulation of Jet Deviation by Rotating Pelton Buckets Using Finite Volume Particle Method, *Transactions of the ASME, Journal of Fluids Engineering*, **137** (7), 074501
[10] Alimirzazadeh S, Jahanbakhsh E, Maertens A, Leguizamón S, Avellan F, GPU-accelerated 3-D Finite Volume Particle Method, Computers and Fluids, **171** (2018) 79–93
[11] Alimirzazadeh S, Kumashiro T, Leguizamon S, Jahanbakhsh E, Maertens A, Vessaz C, Tani K, Avellan F, GPU-accelerated numerical analysis of jet interference in a six-jet Pelton turbine using Finite Volume Particle Method, *Renewable Energy* **148** (2019) 234-246
[12] Bannantine J A, Comer J J, Handrock J L, Fundamental of Fatigue Analysis, Prentice Hall, 1990
[13] Perrig A., Avellan F., Kueny J., Farhat M., Flow in a Pelton Turbine Bucket: Numerical and Experimental Investigations, *Journal of Fluids Engineering* **128** (2006) 350-358